

## Buckling analysis of a size-dependent functionally graded nanobeam resting on Pasternak's foundations

Ashraf Zenkour<sup>1,2,\*</sup>, Farzad Ebrahimi<sup>3</sup>, Mohammad Reza Barati<sup>3</sup>

<sup>1</sup>Department of Mathematics, Faculty of Science, King Abdulaziz University, Jeddah 21589, Saudi Arabia

<sup>2</sup>Department of Mathematics, Faculty of Science, Kafrelsheikh University, Kafrelsheikh 33516, Egypt.

<sup>3</sup>Department of Mechanical Engineering, Faculty of Engineering, Imam Khomeini International University, Qazvin, Iran.

Received 25 August 2018; revised 25 November 2018; accepted 14 December 2018; available online 16 December 2018

### Abstract

Buckling analysis of a functionally graded (FG) nanobeam resting on two-parameter elastic foundation is presented based on third-order shear deformation beam theory (TOSDBT). The in-plane displacement of TOSDBT has parabolic variation through the beam thickness. Also, TOSDBT accounts for shear deformation effect and verifies stress-free boundary conditions on upper and lower faces of FG nanobeam. The two-parameter elastic foundation model including linear Winkler's springs along with Pasternak's shear layer is in contact with the beam in deformation. Material properties of FG nanobeam are supposed to vary gradually along the thickness according to both power-law and Mori-Tanaka laws. Small-scale effect of Eringen's nonlocal elasticity theory has been considered. Nonlocal equilibrium equations are obtained based on the minimum potential energy principle and solved analytically. The accuracy of current method is examined by comparing current results with the available ones in literature. Effects of foundation parameters, gradient index, nonlocal parameter and slenderness ratio on buckling behavior of FG nanobeams are examined.

**Keywords:** Buckling; Elastic Foundation; Functionally Graded (FG); Nanobeam; Nonlocal Elasticity; Third-Order Theory.

### How to cite this article

Zenkour A., Ebrahimi F., Barati MR., Buckling analysis of a size-dependent functionally graded nanobeam resting on Pasternak's foundations. *Int. J. Nano Dimens.*, 2019; 10 (2): 141-153.

### INTRODUCTION

Developments in materials engineering led to the microscopically inhomogeneous spatial composite materials named functionally graded materials (FGMs) which provide huge potential applications for various systems and devices, such as aerospace, aircraft, automobile and defense structures and the electronic devices. According to the fact that FGMs have been placed in category of composite materials, volume fractions of two or more material constituents such as a pair of ceramic-metal are supposed to change smoothly and continuously throughout the gradient directions. FGMs are fabricated to take advantage of desirable features of its constituent phases, for example, in a thermal protection system, the

ceramic constituents are capable to withstand extreme temperature environments due to their better thermal resistance characteristics, while the metal constituents provide stronger mechanical performance and diminishes the possibility of catastrophic fracture. Hence, by presenting novel mechanical properties, FGMs have gained their applicability in many engineering fields, such as biomedical, nuclear, and mechanical engineering.

In addition, fast growing progress in the application of structural elements such as beams, shells and plates with micro/nano length-scale in micro (MEMS) or nano (NEMS) electro-mechanical systems, due to their outstanding chemical, mechanical, and electrical properties, led to a provocation in modelling of micro/nano scale structures. In such applications, the size-

\* Corresponding Author Email: [zenkour@gmail.com](mailto:zenkour@gmail.com)  
[zenkour@kau.edu.sa](mailto:zenkour@kau.edu.sa)

effect has a major role on dynamic response of material. After invention of carbon nanotubes by Iijima [1], nanoscale engineering materials have exposed to considerable attention in modern science and technology. These structures possess extraordinary mechanical, thermal, electrical and chemical performances that are superior to conventional structural materials. Therefore, the analysis of nanostructures attracts great attention by investigators based on molecular dynamics (MD) and continuum mechanics. The problem of classical theory in analysis of nanostructures is that classical continuum mechanics theory does not take care with size-effects in micro- or nano-scale structures. The classical continuum mechanics overpredicts the behaviors of micro-/nano-structures. Another way to capture size-effects is to rely on MD simulations that considered as a powerful and accurate implement to study of structural components at nanoscale. But even the MD simulation at nanoscale is computationally exorbitant for modeling nanostructures with large numbers of atoms. So, a conventional form of continuum mechanics that can capture small-scale effect is required. Eringen's nonlocal continuum theory [2-4] is considered that includes small-scale effects with good accuracy to model micro/nano scale devices and systems. Nonlocal elasticity theory assumes that stress at a reference point is a function of strains at all neighbor points of solid. Hence, this theory could consider effects of small-scales.

For proper design of nanostructures, it is very important to take all essential characteristics of their mechanical behaviors at this submicron size. To achieve this goal, based on nonlocal constitutive equation of Eringen, many studies have been conducted attempting to develop nonlocal beam theories for predicting mechanical behavior of nanobeams. The potential of application of nonlocal Euler-Bernoulli beam theory (EBT) to materials in micro- and nano-scale has been presented by Peddieson *et al.* [5] as the first researcher to perform nonlocal theory to nano structures. Then, nonlocal elasticity theory gained considerable attention among nanotechnology society and utilization of this theory is extended in various mechanical analyses. Reddy [6] presented different available beam theories, containing EBT, Timoshenko's beam theory (TBT), Reddy's, and Levinson's beam theories through nonlocal differential relations of Eringen.

Wang and Liew [7] investigated static response of micro- and nano-scale structures based on nonlocal continuum mechanics using EBT and TBT. Aydogdu [8] employed nonlocal beam theory for bending, buckling, and vibration of nanobeams based on various beam theories. Phadikar and Pradhan [9] used the finite element method and Eringen's theory to discuss bending, vibration, and buckling of beams and Kirchhoff's plates. Civalek *et al.* [10] performed formulation of governing equations of nanobeams to discuss bending of cantilever microtubules based on differential quadrature method. Also, Civalek and Demir [11] proposed a nonlocal EBT to analyze the bending of microtubules. Thai [12] employed nonlocal higher-order beam model to discuss mechanical behavior of nanobeams. Zenkour and his colleagues [13-22] presented the nonlocal Eringen's theory for static and dynamic responses of FG and composite nanobeams.

FG nanostructures are extensively used in MEMS/NEMS due to rapid developments in nanotechnology. Ke and Wang [23] employed small-scale effects on dynamic stability of FG microbeams based on TBT. Recently, Eltahir *et al.* [24] presented static and stability behaviors of FG nanobeams due to nonlocal elasticity theory. Şimşek and Yurtcu [25] performed analytically bending and buckling of FG nanobeam using nonlocal TBT and EBT. Ebrahimi *et al.* [26, 27] discussed applicability of differential transformation method in deducing of vibrational characteristics of FG size-dependent nanobeams. Also, Ebrahimi and Salari [28] investigated a semi-analytical method for vibrational and buckling behavior of FG nanobeams. Niknam and Aghdam [29] also presented natural vibration and buckling response of nonlocal FG beams resting on two-parameter elastic foundation.

Thus, a comprehensive survey in literature reveals that buckling response of FG nanobeams especially for those on elastic foundations are very limited. Various kinds of elastic foundation models for the sake of describing the interactions of the beam and foundation have proposed by scientists. Winkler or one-parameter elastic foundation is known as the simplest model which regards the foundation as a series of separated linear elastic springs without coupling effects between each other. The defect of Winkler's parameter is the behavioral inconsistency associated to discontinuous deflections on interacted surface

area of the beam. Pasternak [30] later introduced an incompressible vertical element as a shear layer which is physically realistic representation of elastic medium and can consider transverse shear stresses due to interaction of shear deformation of surrounding elastic medium. Thus, a more realistic and generalized representation of elastic foundation is expected through a two-parameter foundation model.

Reddy's beam theory [6] relaxes the limitation on the warping of the cross sections and allows cubic variations in the longitudinal direction of the beam, so it can produce adequate accuracy when applying for beam analysis. However, a few studies have been made to present mechanical behavior of FG micro/nanobeams by using higher-order and sinusoidal (Touratier [31]) beam theories. Rahmani and Jandaghian [32] employed buckling response of FG nanobeams based on a nonlocal TOSDBT. Sahmani *et al.* [33] employed free vibration of FG nanobeams around postbuckling domain incorporating effects of surface free energy. Şimşek and Reddy [34] presented buckling of FG microbeam resting on two-parameter Pasternak's foundation using modified couple stress and unified higher-order beam theories. Zhang *et al.* [35] developed a size-dependent FG beam resting on two-parameter foundation based on an improved TOSDBT and provided analytical solutions for bending, buckling and free vibration problems. Microstructure buckling analysis of FG third-order microbeams in thermal environment has been performed via modified strain gradient theory by Sahmani and Ansari [36]. It is to be noted until now that a work analyzing buckling behavior of embedded FG nanobeams using the TOSDBT has not been yet presented.

In the current article, the non-classical TOSDBT is developed for buckling of FG nanobeam

embedded on elastic foundations. Material properties of FG nanobeam will be continuously changed along the beam thickness according to two kinds of micromechanics models, namely, power-law and Mori-Tanaka models. By using the minimum potential energy principle, equilibrium equations are obtained and Navier-type solution is used to solve them. The obtained results based on TOSDBT are compared with those predicted in previously published works to verify the accuracy of the current solution. Numerical results are reported to discuss effects of gradient index, nonlocality and foundation parameters on buckling response of FG nanobeams.

### MATERIALS AND METHODS

#### Power-law and Mori-Tanaka FGM beam models

The FG nanobeam (shown in Fig. 1) is graded according to two models. Firstly, the power-law (PL) model for FGMs can be represented as:

$$P_f = P_c V_c + P_m V_m, \quad V_c + V_m = 1, \quad (1)$$

in which  $P_f(z)$  is the effective material property of the FG beam, subscripts  $m$  and  $c$  represent metal and ceramic, respectively,  $V_m$  and  $V_c$  represent volume fractions of metal and ceramic, respectively. The effective material properties such as Young's modulus and Poisson's ratio of FG nanobeam are expressed as:

$$E(z) = (E_c - E_m) \left( \frac{z}{h} + \frac{1}{2} \right)^p + E_m, \quad (2)$$

$$\nu(z) = (\nu_c - \nu_m) \left( \frac{z}{h} + \frac{1}{2} \right)^p + \nu_m,$$

in which  $p$  represents power-law exponent that determines material distribution through the nanobeam thickness.

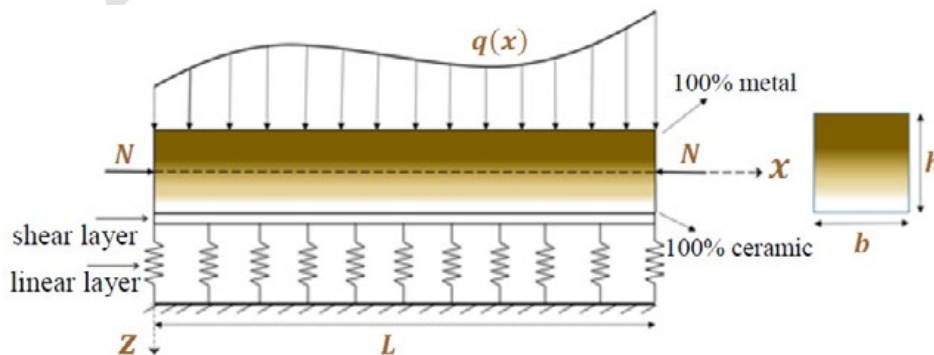


Fig. 1. Geometry and coordinates of FG nanobeam resting on elastic foundation.

Secondly, Mori-Tanaka (MT) homogenization technique is also utilized to model effective material properties of the current FG nanobeam. According to MT the effective local bulk modulus  $K_e$  and shear modulus  $\mu_e$  can be represented as (Şimşek and Reddy [34]):

$$\frac{K_e - K_m}{K_c - K_m} = \frac{V_c}{1 + \frac{V_m(K_c - K_m)}{K_m + \frac{4}{3}\mu_m}},$$

$$\frac{\mu_e - \mu_m}{\mu_c - \mu_m} = \frac{V_c}{1 + \frac{V_m(\mu_c - \mu_m)}{\mu_m + \frac{\mu_m(9K_m + 8\mu_m)}{9(K_m + 2\mu_m)}}}. \quad (3)$$

Therefore from Eq. (3), based on MT scheme, Young's modulus and Poisson's ratio can be represented by:

$$E(z) = \frac{9K_e\mu_e}{3K_e + \mu_e}, \quad \nu(z) = \frac{3K_e - 2\mu_e}{6K_e + 2\mu_e}. \quad (4)$$

The shear modulus  $G(z)$  of FG nanobeam is defined by:

$$G(z) = \frac{E(z)}{2[1 + \nu(z)]}. \quad (5)$$

**Kinematic relations**

The displacement field of TOSDBT at any point of nanobeam is given by

$$u_x(x, z) = u(x) + z\varphi(x) - \alpha z^3 \left( \varphi + \frac{\partial w}{\partial x} \right),$$

$$u_z(x, z) = w(x), \quad (6)$$

in which  $\alpha = \frac{4}{3h^2}$ ,  $u$  and  $w$  represent longitudinal and transverse displacements,  $\varphi$  represents rotation of cross section at each point of neutral axis. Cauchy's relations of Reddy's beam model are given by

$$\varepsilon_{xx} = \varepsilon_{xx}^{(0)} + z\varepsilon_{xx}^{(1)} + z^3\varepsilon_{xx}^{(3)}, \quad \gamma_{xz} = \gamma_{xz}^{(0)} + z^2\gamma_{xz}^{(2)}. \quad (7)$$

where

$$\varepsilon_{xx}^{(0)} = \frac{\partial u}{\partial x}, \quad \varepsilon_{xx}^{(1)} = \frac{\partial \varphi}{\partial x}, \quad \varepsilon_{xx}^{(3)} = -\alpha \left( \frac{\partial \varphi}{\partial x} + \frac{\partial^2 w}{\partial x^2} \right),$$

$$\gamma_{xz}^{(0)} = \varphi + \frac{\partial w}{\partial x}, \quad \gamma_{xz}^{(2)} = -\beta \left( \varphi + \frac{\partial w}{\partial x} \right), \quad (8)$$

and  $\beta = \frac{4}{h^2}$ .

By using the extremum condition of the

minimum potential energy principle in the form

$$\delta(U + V) = 0. \quad (9)$$

Here  $U$  denotes strain energy and  $V$  denotes work done by external forces. The virtual strain energy is represented by:

$$\delta U = \iiint_V \sigma_{ij} \delta \varepsilon_{ij} dv = \iiint_V (\sigma_{xx} \delta \varepsilon_{xx} + \sigma_{xz} \delta \gamma_{xz}) dv. \quad (10)$$

Using Eq. (7) into Eq. (10) gives

$$\delta U = \int_0^L (N \delta \varepsilon_{xx}^{(0)} + M \delta \varepsilon_{xx}^{(1)} + P \delta \varepsilon_{xx}^{(3)} + Q \delta \gamma_{xz}^{(0)} + R \delta \gamma_{xz}^{(2)}) dx, \quad (11)$$

in which

$$\{N, M, P\} = \iint_A \sigma_{xx} \{1, z, z^3\} dA,$$

$$\{Q, R\} = \iint_A \sigma_{xz} \{1, z^2\} dA. \quad (12)$$

Also

$$\delta V = \int_0^L \left[ \left( \mathcal{N} \frac{\partial w}{\partial x} \frac{\partial}{\partial x} + q - k_w + k_p \frac{\partial^2}{\partial x^2} + \alpha P \frac{\partial^2}{\partial x^2} \right) \delta w \right. \\ \left. + f \delta u - N \delta \varepsilon_{xx}^{(0)} - \bar{M} \frac{\partial \delta \varphi}{\partial x} - \bar{Q} \delta \gamma_{xz}^{(0)} \right] dx, \quad (13)$$

in which  $\bar{M} = M - \alpha P$ ,  $\bar{Q} = Q - \beta R$ ,  $\mathcal{N}$  represents applied axial compressive load,  $q$  and  $f$  are transverse and axial distributed loadings and  $k_w$  and  $k_p$  are linear and shear parameters of elastic foundation.

By using Eqs. (11) and (13) into Eq. (9) and setting coefficients of  $\delta u$ ,  $\delta w$  and  $\delta \varphi$  to zero, the following Euler-Lagrange equations may be represented as:

$$\frac{\partial N}{\partial x} + f = 0, \quad \frac{\partial \bar{M}}{\partial x} - \bar{Q} = 0, \quad (14)$$

$$\frac{\partial \bar{Q}}{\partial x} - \mathcal{N} \frac{\partial^2 w}{\partial x^2} + \alpha \frac{\partial^2 P}{\partial x^2} + q - k_w w + k_p \frac{\partial^2 w}{\partial x^2} = 0.$$

**Nonlocal elasticity model for FG nanobeam**

According to Eringen's nonlocal elasticity model (Eringen and Edelen [2]), the stresses  $\sigma_{ij}$  at each point  $x$  in the solid may be represented by

$$\sigma_{ij}(x) = \iiint_V \psi(|x - x'|, \tau) t_{ij}(x') dv(x'), \quad (15)$$

in which  $t_{ij}(x')$  represent components available in local stress tensor at point  $x$  which are associated to strain tensor components  $\varepsilon_{kl}$  as



$$t_{ij} = C_{ijkl} \varepsilon_{kl}. \quad (16)$$

In Eq. (15), the size that is related to nonlocal kernel  $\psi(|x-x'|, \tau)$  and  $|x-x'|$  is Euclidean distance and  $\tau = e_0 a / l$  is a constant in which  $a$  is internal length,  $l$  is a characteristic external length, and  $e_0$  is experimentally estimated. The integral constitutive equations appeared in Eq. (16) in an equivalent differential form is represented by:

$$\left[1 - (e_0 a)^2 \nabla^2\right] \sigma_{kl} = t_{kl}, \quad (17)$$

in which  $\nabla^2$  represents Laplacian operator. For a 1D material, the constitutive relations of nonlocal theory may be represented by:

$$\begin{aligned} \sigma_{xx} - (e_0 a)^2 \frac{\partial^2 \sigma_{xx}}{\partial x^2} &= E \varepsilon_{xx}, \\ \sigma_{xz} - (e_0 a)^2 \frac{\partial^2 \sigma_{xz}}{\partial x^2} &= G \gamma_{xz}, \end{aligned} \quad (18)$$

where  $\sigma$  and  $\varepsilon$  represent nonlocal stress and strain, respectively. For a nonlocal FG beam, Eqs. (18) is expressed as

$$\begin{aligned} \sigma_{xx} - \mu \frac{\partial^2 \sigma_{xx}}{\partial x^2} &= E(z) \varepsilon_{xx}, \\ \sigma_{xz} - \mu \frac{\partial^2 \sigma_{xz}}{\partial x^2} &= G(z) \gamma_{xz}, \end{aligned} \quad (19)$$

in which  $\mu = (e_0 a)^2$ . Integrating Eqs. (19) over cross-section area, we obtain

$$N - \mu \frac{\partial^2 N}{\partial x^2} = A_{xx} \frac{\partial u}{\partial x} + (B_{xx} - \alpha E_{xx}) \frac{\partial \varphi}{\partial x} - \alpha E_{xx} \frac{\partial^2 w}{\partial x^2}, \quad (20)$$

$$M - \mu \frac{\partial^2 M}{\partial x^2} = B_{xx} \frac{\partial u}{\partial x} + (D_{xx} - \alpha F_{xx}) \frac{\partial \varphi}{\partial x} - \alpha F_{xx} \frac{\partial^2 w}{\partial x^2}, \quad (21)$$

$$P - \mu \frac{\partial^2 P}{\partial x^2} = E_{xx} \frac{\partial u}{\partial x} + (F_{xx} - \alpha H_{xx}) \frac{\partial \varphi}{\partial x} - \alpha H_{xx} \frac{\partial^2 w}{\partial x^2}, \quad (22)$$

$$Q - \mu \frac{\partial^2 Q}{\partial x^2} = (A_{xz} - \beta D_{xz}) \left( \frac{\partial w}{\partial x} + \varphi \right), \quad (23)$$

$$R - \mu \frac{\partial^2 R}{\partial x^2} = (D_{xz} - \beta F_{xz}) \left( \frac{\partial w}{\partial x} + \varphi \right), \quad (24)$$

where the cross-sectional rigidities are given by:

$$\begin{aligned} \{A_{xx}, B_{xx}, D_{xx}, E_{xx}, F_{xx}, H_{xx}\} &= \\ \int_{-h/2}^{h/2} E(z) \{1, z, z^2, z^3, z^4, z^6\} dz, & \quad (25) \end{aligned}$$

$$\{A_{xz}, D_{xz}, F_{xz}\} = \int_{-h/2}^{h/2} G(z) \{1, z^2, z^4\} dz. \quad (26)$$

The nonlocal normal force is obtained by using second derivative of  $N$  from Eq. (14)<sub>1</sub> into Eq. (20) as

$$N = A_{xx} \frac{\partial u}{\partial x} + K_{xx} \frac{\partial \varphi}{\partial x} - \alpha E_{xx} \frac{\partial^2 w}{\partial x^2} - \mu \frac{\partial^2 N}{\partial x^2}. \quad (27)$$

Eliminating  $\bar{Q}$  from Eqs. (14)<sub>2</sub> and (14)<sub>3</sub> yields

$$\frac{\partial^2 \bar{M}}{\partial x^2} = \mathcal{N} \frac{\partial^2 w}{\partial x^2} - \alpha \frac{\partial^2 P}{\partial x^2} - q + k_w w - k_p \frac{\partial^2 w}{\partial x^2}. \quad (28)$$

Also, the nonlocal bending moment can be derived by using the above equation into Eqs. (21) and (22) as follows:

$$\begin{aligned} \bar{M} &= K_{xx} \frac{\partial u}{\partial x} + I_{xx} \frac{\partial \varphi}{\partial x} - \alpha J_{xx} \left( \frac{\partial^2 w}{\partial x^2} + \frac{\partial \varphi}{\partial x} \right) \\ &+ \mu \left( \mathcal{N} \frac{\partial^2 w}{\partial x^2} - \alpha \frac{\partial^2 P}{\partial x^2} - q + k_w w - k_p \frac{\partial^2 w}{\partial x^2} \right), \end{aligned} \quad (29)$$

Where

$$K_{xx} = B_{xx} - \alpha E_{xx}, \quad I_{xx} = D_{xx} - \alpha F_{xx}, \quad J_{xx} = F_{xx} - \alpha H_{xx}. \quad (30)$$

The substitution of second derivative of the nonlocal shear force  $\bar{Q}$  from Eq. (14)<sub>3</sub> into Eq. (23) with the aid of Eq. (24) yields  $\bar{Q}$  in the form

$$\begin{aligned} \bar{Q} &= A_{xz}^* \left( \frac{\partial w}{\partial x} + \varphi \right) \\ \bar{M} &= K_{xx} \frac{\partial u}{\partial x} + I_{xx} \frac{\partial \varphi}{\partial x} - \alpha J_{xx} \left( \frac{\partial^2 w}{\partial x^2} + \frac{\partial \varphi}{\partial x} \right) \end{aligned} \quad (31)$$

Where

$$A_{xz}^* = \bar{A}_{xz} - \beta \bar{D}_{xz}, \quad \bar{A}_{xz} = A_{xz} - \beta D_{xz}, \quad \bar{D}_{xz} = D_{xz} - \beta F_{xz}. \quad (32)$$

using  $\bar{M}$  and  $\bar{Q}$  from Eqs. (29) and (31) and the identity that given from Eq. (22) to get

$$\begin{aligned} \alpha \frac{\partial^2}{\partial x^2} \left( P - \mu \frac{\partial^2 P}{\partial x^2} \right) \\ = \alpha E_{xx} \frac{\partial^3 u}{\partial x^3} + \alpha J_{xx} \frac{\partial^3 \varphi}{\partial x^3} - \alpha^2 H_{xx} \frac{\partial^4 w}{\partial x^4}. \end{aligned} \quad (33)$$

The nonlocal governing equations of FG nanobeam in terms of displacement can be obtained by substituting for  $N$ ,  $\bar{M}$  and  $\bar{Q}$  from Eqs. (27), (29) and (31), respectively, and using Eq. (33) into Eqs. (14) as follows:

$$A_{xx} \frac{\partial^2 u}{\partial x^2} + K_{xx} \frac{\partial^2 \varphi}{\partial x^2} - \alpha E_{xx} \frac{\partial^3 w}{\partial x^3} - \mu \frac{\partial^2 f}{\partial x^2} + f = 0, \quad (34)$$

$$K_{xx} \frac{\partial^2 u}{\partial x^2} + I_{xx} \frac{\partial^2 \varphi}{\partial x^2} - \alpha J_{xx} \left( \frac{\partial^3 w}{\partial x^3} + \frac{\partial^2 \varphi}{\partial x^2} \right)$$

$$-A_{xz}^* \left( \frac{\partial w}{\partial x} + \varphi \right) = 0, \quad (35)$$

$$A_{xz}^* \left( \frac{\partial^2 w}{\partial x^2} + \frac{\partial \varphi}{\partial x} \right) + \mu \left( \mathcal{N} \frac{\partial^4 w}{\partial x^4} - \frac{\partial^2 q}{\partial x^2} + k_w \frac{\partial^2 w}{\partial x^2} - k_p \frac{\partial^4 w}{\partial x^4} \right) \\ - \mathcal{N} \frac{\partial^3 w}{\partial x^3} + q - k_w w + k_p \frac{\partial^3 w}{\partial x^3} + \alpha E_{xx} \frac{\partial^3 u}{\partial x^3} + \alpha J_{xx} \frac{\partial^3 \varphi}{\partial x^3} \quad (36) \\ - \alpha^2 H_{xx} \frac{\partial^4 w}{\partial x^4} = 0.$$

**RESULTS AND DISCUSSIONS**

The displacement field that satisfy the simply-supported boundary conditions is represented as

$$\begin{Bmatrix} u(x,t) \\ w(x,t) \\ \varphi(x,t) \end{Bmatrix} = \sum_{n=1}^{\infty} \begin{Bmatrix} U_n \cos\left(\frac{n\pi}{L}x\right) \\ W_n \sin\left(\frac{n\pi}{L}x\right) \\ \Phi_n \cos\left(\frac{n\pi}{L}x\right) \end{Bmatrix} e^{i\omega_n t}, \quad (37)$$

in which  $U_n$ ,  $W_n$  and  $\Phi_n$  denote unknown Fourier’s coefficients to be determined for each  $n$ . It is to be noted that the conditions for simply-supported beam are expressed as

$$u(0,t) = 0, \quad \frac{\partial u}{\partial x} \Big|_{x=L} = 0, \quad w(0,t) = w(L,t) = 0, \\ \frac{\partial \varphi}{\partial x} \Big|_{x=0} = \frac{\partial \varphi}{\partial x} \Big|_{x=L} = 0. \quad (38)$$

Using Eqs. (37) into Eqs. (34)-(36), respectively, leads to

$$-A_{xx} \left( \frac{n\pi}{L} \right)^2 U_n - K_{xx} \left( \frac{n\pi}{L} \right)^2 \Phi_n + \alpha E_{xx} \left( \frac{n\pi}{L} \right)^3 W_n = 0, \quad (39)$$

$$-K_{xx} \left( \frac{n\pi}{L} \right)^2 U_n - \left[ I_{xx} \left( \frac{n\pi}{L} \right)^2 - \alpha J_{xx} \left( \frac{n\pi}{L} \right)^2 + A_{xz}^* \right] \Phi_n \\ + \frac{n\pi}{L} \left[ \alpha J_{xx} \left( \frac{n\pi}{L} \right)^2 - A_{xz}^* \right] W_n = 0, \quad (40)$$

$$\alpha E_{xx} \left( \frac{n\pi}{L} \right)^3 U_n + \frac{n\pi}{L} \left[ \alpha J_{xx} \left( \frac{n\pi}{L} \right)^2 - A_{xz}^* \right] \Phi_n \\ - \left[ \bar{A}_{xz} \left( \frac{n\pi}{L} \right)^2 + \alpha^2 H_{xx} \left( \frac{n\pi}{L} \right)^4 + \left[ 1 + \mu \left( \frac{n\pi}{L} \right)^2 \right] \right] \quad (41)$$

$$\left[ k_w + k_p \left( \frac{n\pi}{L} \right)^2 - \mathcal{N} \left( \frac{n\pi}{L} \right)^2 \right] W_n = 0.$$

Table 1. Material properties of FGM constituents.

Properties	Steel	Alumina (Al <sub>2</sub> O <sub>3</sub> )
$E$	210 GPa	390 GPa
$\nu$	0.3	0.3

The above equations may be summarized as:

$$[K]\{\Delta\} = \{0\}, \quad (42)$$

where  $\{\Delta\} = \{U_n, W_n, \Phi_n\}^T$  and  $[K]$  is stiffness matrix. By putting this polynomial to zero, we can find buckling loads.

Here, effects of FG distribution, nonlocality effect and mode number on natural frequencies of FG nanobeam are presented. The FG nanobeam is a combination of *steel* and *alumina* (Al<sub>2</sub>O<sub>3</sub>) where their properties are reported in Table 1. The following dimensions for the beam geometry is considered:  $L$  (length) = 10<sup>4</sup> nm,  $b$  (width) = 10<sup>3</sup> nm (Eltaher *et al.* [37]; Rahmani and Pedram [38]). In addition, for better presentation of results the following dimensionless quantities are adopted (Şimşek and Reddy [34]):

$$N_{cr} = \mathcal{N} \frac{L^2}{E_m I}, \quad K_w = k_w \frac{L^4}{E_m I}, \quad K_p = k_p \frac{L^2}{E_m I}. \quad (43)$$

where  $I = bh^3 / 12$  represents moment inertia of beam’s cross-section. For verification purpose, dimensionless buckling loads of simply-supported FG nanobeam with different nonlocal parameters and gradient indexes are compared with results reported in Eltaher *et al.* [37] and Rahmani and Jandaghian [32] for nonlocal EBT and nonlocal Reddy’s beam theory, respectively. In these work, the variation of Poisson’s ratio along the beam thickness is not considered and it is fixed to be 0.3. It can be observed from Table 2 that results of nonlocal Reddy’s beam theory are smaller than those of nonlocal EBT. This is attributed to the fact that Euler–Bernoulli’s beam model is unable to capture the influence of shear deformation.

The variation of dimensionless buckling loads of FG nanobeam for both PL and MT models with different gradient indexes ( $p = 0, 0.5, 1, 5$ ), nonlocal parameters, foundation parameters and slenderness ratios are presented in Tables 3-5. The present results for MT model and PL model are referred to as MT-FGM and PL-FGM, respectively. It can be noticed from the tables that non-dimensional buckling loads predicted





Table 2. Comparison of dimensionless buckling load for a S-S FG nanobeam with various gradient indexes without elastic foundation ( $L/h = 20$ ).

$p$	$\mu = 1$				$\mu = 2$		
	EBT (Eltaher et al. [24])	RBT and [32])	(Rahmani Jandaghian,	Present	EBT (Eltaher et al. [24])	RBT (Rahmani and Jandaghian, [32])	Present
0	8.9843		8.9258	8.925759	8.2431	8.1900	8.190046
0.1	10.1431		9.7778	9.777865	9.2356	8.9719	8.971916
0.2	10.2614		10.3898	10.389845	9.7741	9.5334	9.533453
0.5	11.6760		11.4944	11.494448	10.6585	10.5470	10.547009
1	12.4581		12.3709	12.370918	12.0652	11.3512	11.351234
2	13.1254		13.1748	13.174885	12.4757	12.0889	12.088934
5	13.5711		14.2363	14.236343	13.2140	13.0629	13.062900
$p$	$\mu = 3$				$\mu = 4$		
	EBT (Eltaher et al. [24])	RBT and [32])	(Rahmani Jandaghian,	Present	EBT (Eltaher et al. [24])	RBT (Rahmani and Jandaghian, [32])	Present
0	7.6149		7.5663	7.566381	7.0765	7.0309	7.030978
0.1	8.5786		8.2887	8.288712	8.0416	7.7021	7.702196
0.2	9.3545		8.8074	8.807489	8.3176	8.1842	8.184264
0.5	9.8093		9.7438	9.743863	9.0585	9.0543	9.054379
1	10.9776		10.4869	10.486847	9.9816	9.7447	9.744790
2	11.7415		11.1683	11.168372	10.4649	10.3781	10.378089
5	12.2786		12.0682	12.068171	11.5231	11.2142	11.214218

Table 3. The variation of nondimensional buckling loads of S-S FG nanobeam with various gradient indexes and nonlocal parameters ( $K_p = 0, L/h = 20$ ).

$K_w$	$\mu$	Gradient index ( $p$ )							
		0		0.5		1		5	
		PL-FGM	MT-FGM	PL-FGM	MT-FGM	PL-FGM	MT-FGM	PL-FGM	MT-FGM
0	0	9.8067	9.8067	12.6289	12.3794	13.5919	13.3665	15.6414	15.4096
	1	8.92576	8.92576	11.4944	11.2673	12.3709	12.1657	14.2363	14.0254
	2	8.19005	8.19005	10.5470	10.3386	11.3512	11.1630	13.0629	12.8693
	3	7.56638	7.56638	9.74386	9.55132	10.4868	10.3129	12.0682	11.8894
	4	7.03098	7.03098	9.05438	8.87546	9.74479	9.58317	11.2142	11.0481
25	0	12.3397	12.3397	15.1619	14.9124	16.1249	15.8995	18.1744	17.9427
	1	11.4588	11.4588	14.0275	13.8003	14.9039	14.6988	16.7694	16.5584
	2	10.7231	10.7231	13.0800	12.8716	13.8843	13.6960	15.5959	15.4024
	3	10.0994	10.0994	12.2769	12.0844	13.0199	12.8460	14.6012	14.4224
	4	9.56401	9.56401	11.5874	11.4085	12.2778	12.1162	13.7472	13.5811
50	0	14.8728	14.8728	17.6950	17.4454	18.6579	18.4325	20.7075	20.4757
	1	13.9918	13.9918	16.5605	16.3334	17.4370	17.2318	19.3024	19.0915
	2	13.2561	13.2561	15.6131	15.4047	16.4173	16.2290	18.1290	17.9354
	3	12.6324	12.6324	14.8099	14.6174	15.5529	15.3790	17.1342	16.9554
	4	12.0970	12.0970	14.1204	13.9415	14.8108	14.6492	16.2803	16.1141
100	0	19.9388	19.9388	22.7610	22.5115	23.7240	23.4986	25.7735	25.5418
	1	19.0579	19.0579	21.6266	21.3994	22.5030	22.2979	24.3685	24.1575
	2	18.3222	18.3222	20.6791	20.4707	21.4834	21.2951	23.1950	23.0015
	3	17.6985	17.6985	19.8760	19.6834	20.6190	20.4450	22.2003	22.0215
	4	17.1631	17.1631	19.1865	19.0076	19.8769	19.7153	21.3463	21.1802

with respect to PL model are larger than that of MT homogenization scheme, related to the fact that for a constant gradient index, FG nanobeam becomes more flexible based on MT homogenization scheme compared to the PL model. The obtained results using MT and PL models are the same at  $p = 0$  since nanobeam is fully ceramic. From this point of view, the

difference between results of these two models is significant when gradient index value is more than zero. Considering explanations and according to Tables 3-5, it must be noted that, as gradient index increases dimensionless buckling load increases (constant nonlocal parameter) too. In addition, at a fixed gradient index the dimensionless buckling load decreases as nonlocal parameter increases.



Table 4. The variation of the nondimensional buckling loads of S-S FG nanobeam with various gradient indexes and nonlocal parameters ( $K_p = 5, L/h = 20$ ).

$K_W$	$\mu$	Gradient index ( $p$ )							
		0		0.5		1		5	
		PL-FGM	MT-FGM	PL-FGM	MT-FGM	PL-FGM	MT-FGM	PL-FGM	MT-FGM
0	0	14.8067	14.8067	17.6289	17.3794	18.5919	18.3665	20.6414	20.4096
	1	13.9258	13.9258	16.4944	16.2673	17.3709	17.1657	19.2363	19.0254
	2	13.1900	13.1900	15.5470	15.3386	16.3512	16.1630	18.0629	17.8693
	3	12.5664	12.5664	14.7439	14.5513	15.4868	15.3129	17.0682	16.8894
	4	12.0310	12.0310	14.0544	13.8755	14.7448	14.5832	16.2142	16.0481
25	0	17.3397	17.3397	20.1619	19.9124	21.1249	20.8995	23.1744	22.9427
	1	16.4588	16.4588	19.0275	18.8003	19.9039	19.6988	21.7694	21.5584
	2	15.7231	15.7231	18.0800	17.8716	18.8843	18.6960	20.5959	20.4024
	3	15.0994	15.0994	17.2769	17.0844	18.0199	17.8460	19.6012	19.4224
	4	14.5640	14.564	16.5874	16.4085	17.2778	17.1162	18.7472	18.5811
50	0	19.8728	19.8728	22.6950	22.4454	23.6579	23.4325	25.7075	25.4757
	1	18.9918	18.9918	21.5605	21.3334	22.4370	22.2318	24.3024	24.0915
	2	18.2561	18.2561	20.6131	20.4047	21.4173	21.2290	23.129	22.9354
	3	17.6324	17.6324	19.8099	19.6174	20.5529	20.3790	22.1342	21.9554
	4	17.0970	17.0970	19.1204	18.9415	19.8108	19.6492	21.2803	21.1141
100	0	24.9388	24.9388	27.7610	27.5115	28.7240	28.4986	30.7735	30.5418
	1	24.0579	24.0579	26.6266	26.3994	27.5030	27.2979	29.3685	29.1575
	2	23.3222	23.3222	25.6791	25.4707	26.4834	26.2951	28.1950	28.0015
	3	22.6985	22.6985	24.8760	24.6834	25.6190	25.4450	27.2003	27.0215
	4	22.1631	22.1631	24.1865	24.0076	24.8769	24.7153	26.3463	26.1802

Table 5. The variation of dimensionless buckling loads of S-S FG nanobeam with various gradient indexes and nonlocal parameters ( $K_p = 10, L/h = 20$ ).

$K_W$	$\mu$	Gradient index ( $p$ )							
		0		0.5		1		5	
		PL-FGM	MT-FGM	PL-FGM	MT-FGM	PL-FGM	MT-FGM	PL-FGM	MT-FGM
0	0	19.8067	19.8067	22.6289	22.3794	23.5919	23.3665	25.6414	25.4096
	1	18.9258	18.9258	21.4944	21.2673	22.3709	22.1657	24.2363	24.0254
	2	18.1900	18.1900	20.5470	20.3386	21.3512	21.1630	23.0629	22.8693
	3	17.5664	17.5664	19.7439	19.5513	20.4868	20.3129	22.0682	21.8894
	4	17.0310	17.0310	19.0544	18.8755	19.7448	19.5832	21.2142	21.0481
25	0	22.3397	22.3397	25.1619	24.9124	26.1249	25.8995	28.1744	27.9427
	1	21.4588	21.4588	24.0275	23.8003	24.9039	24.6988	26.7694	26.5584
	2	20.7231	20.7231	23.0800	22.8716	23.8843	23.6960	25.5959	25.4024
	3	20.0994	20.0994	22.2769	22.0844	23.0199	22.8460	24.6012	24.4224
	4	19.5640	19.5640	21.5874	21.4085	22.2778	22.1162	23.7472	23.5811
50	0	24.8728	24.8728	27.6950	27.4454	28.6579	28.4325	30.7075	30.4757
	1	23.9918	23.9918	26.5605	26.3334	27.4370	27.2318	29.3024	29.0915
	2	23.2561	23.2561	25.6131	25.4047	26.4173	26.2290	28.1290	27.9354
	3	22.6324	22.6324	24.8099	24.6174	25.5529	25.3790	27.1342	26.9554
	4	22.0970	22.0970	24.1204	23.9415	24.8108	24.6492	26.2803	26.1141
100	0	29.9388	29.9388	32.7610	32.5115	33.7240	33.4986	35.7735	35.5418
	1	29.0579	29.0579	31.6266	31.3994	32.5030	32.2979	34.3685	34.1575
	2	28.3222	28.3222	30.6791	30.4707	31.4834	31.2951	33.1950	33.0015
	3	27.6985	27.6985	29.8760	29.6834	30.6190	30.4450	32.2003	32.0215
	4	27.1631	27.1631	29.1865	29.0076	29.8769	29.7153	31.3463	31.1802

Furthermore, it should be stated that when the foundation parameters (Winkler's and Pasternak's parameter) increase, the non-dimensional buckling load increases which indicates the stiffening effect

of foundation parameters on the FG nanobeam.

The effect of elastic foundation on non-dimensional buckling load of FG nanobeam with varying of gradient index at  $L/h = 20$  is presented





in Fig. 2(a, b) and the variation of non-dimensional buckling load with and without elastic foundation based on both PL and MT models are compared. It is seen from the results of this figure that the dimensionless buckling loads of FG nanobeam embedded in elastic medium are larger than that of FG nanobeam without elastic foundation. This is since when the both foundation parameters increase the nanobeam becomes stiffer. Also, the MT scheme estimates lower values for the non-dimensional buckling loads compared to the power-law model. The reason is that, MT model provides smaller values for Young's modulus than the power-law model and thus leads to a more flexible structure. Also, it is noticed from this figure that the dimensionless buckling load is

prominently affected by lower values of gradient indexes. Also, increasing nonlocal parameter shows a decreasing effect on the dimensionless buckling load. So, as a general consequence, the presence of nonlocality and elastic foundation softens and stiffens the structure, respectively.

Fig. 3(a, b) shows variation of dimensionless buckling load of FG nanobeam with respect to slenderness ratio (at  $K_w = 25$  and  $K_p = 5$ ) for various values of gradient indexes used in MT model as well as PL model. It is seen that, dimensionless buckling load increases with increase in slenderness ratio. But this observation is accurate when slenderness ratio is in the range  $L/h < 20$ . Therefore, it can be deduced that effect of slenderness ratio on dimensionless buckling

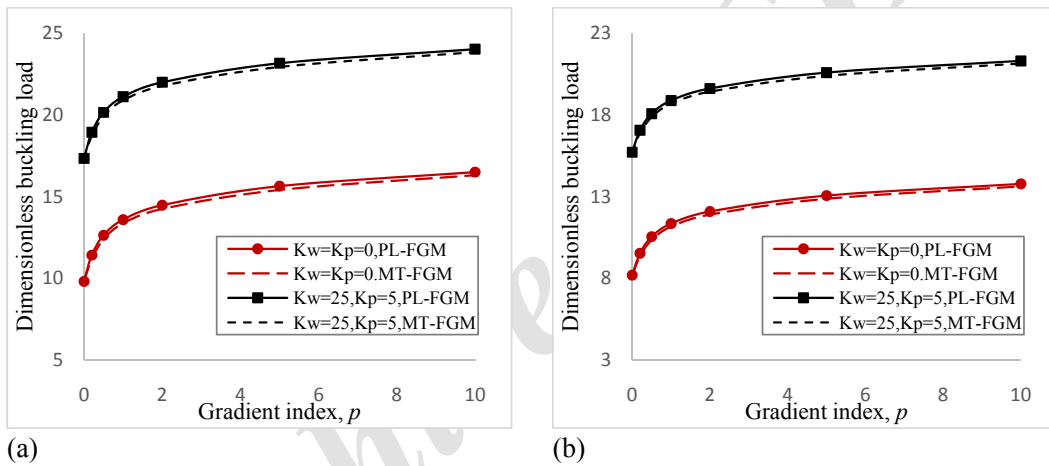


Fig. 2. The effect of presence of elastic foundation on dimensionless buckling load of FG nanobeam based on power-law and Mori-Tanaka models with gradient index when  $L/h = 20$ ; (a)  $\mu = 0$ , (b)  $\mu = 2$ .

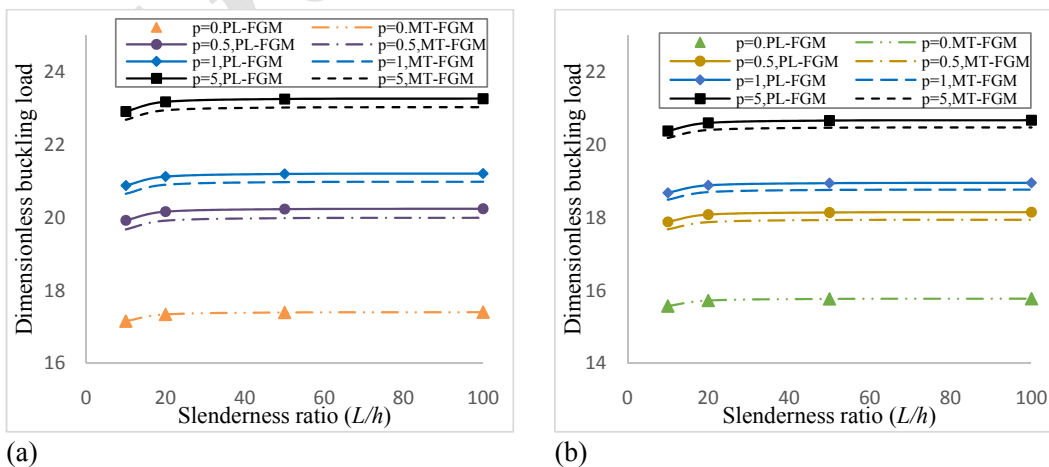


Fig. 3. The comparison of dimensionless buckling load versus slenderness ratio for different gradient indexes when  $K_p = 5$ ,  $K_w = 25$ ; (a) classical beam theory  $\mu = 0$ . (b) Nonlocal beam theory  $\mu = 2$ .



load is approximately diminishes for values greater than  $L/h > 20$ .

The softening effect of nonlocal parameter on the dimensionless buckling load of S-S FG nanobeams for various gradient indexes at  $L/h = 20$  with and without elastic foundation is shown in Fig. 4(a, b), so as nonlocal parameter

grows, dimensionless buckling load reduces for all gradient indexes.

The variation of dimensionless buckling load of S-S FG nanobeam with Winkler's parameter for different nonlocal parameters and gradient indexes is presented in Fig 5(a-d). In this figure, the MT model is adopted. It is seen that with increase

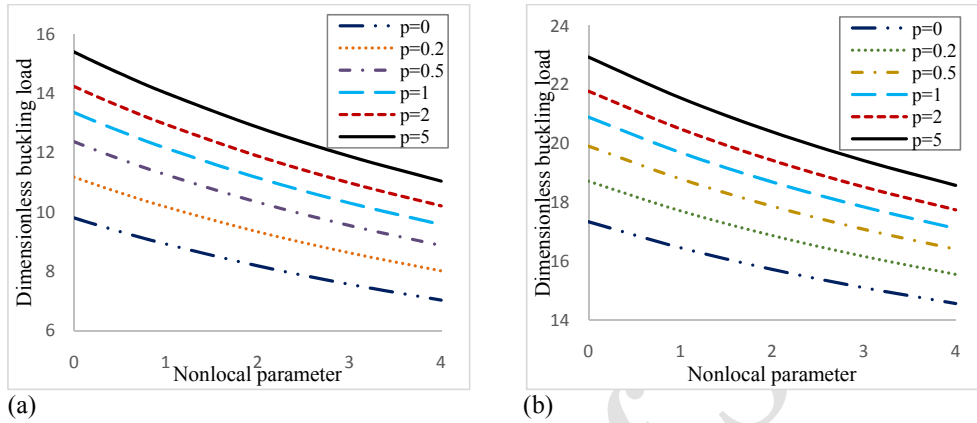


Fig. 4. The variation of dimensionless buckling load of FG nanobeam with nonlocal parameter and gradient index at  $L/h = 20$ ; (a)  $K_W = K_p = 0$ , (b)  $K_W = 25, K_p = 5$ .

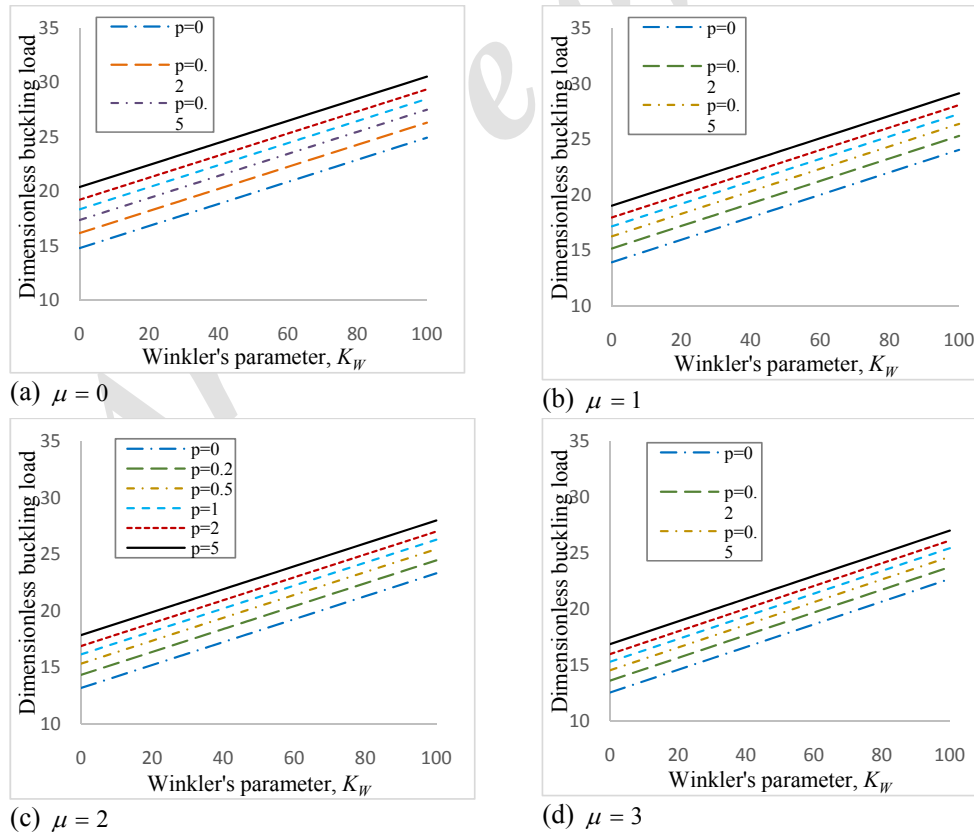


Fig. 5 (a, b, c, d). The variation of dimensionless buckling load of FG nanobeam with Winkler's parameter and gradient index for different nonlocal parameters at  $L/h = 20$  and  $K_p = 5$ .



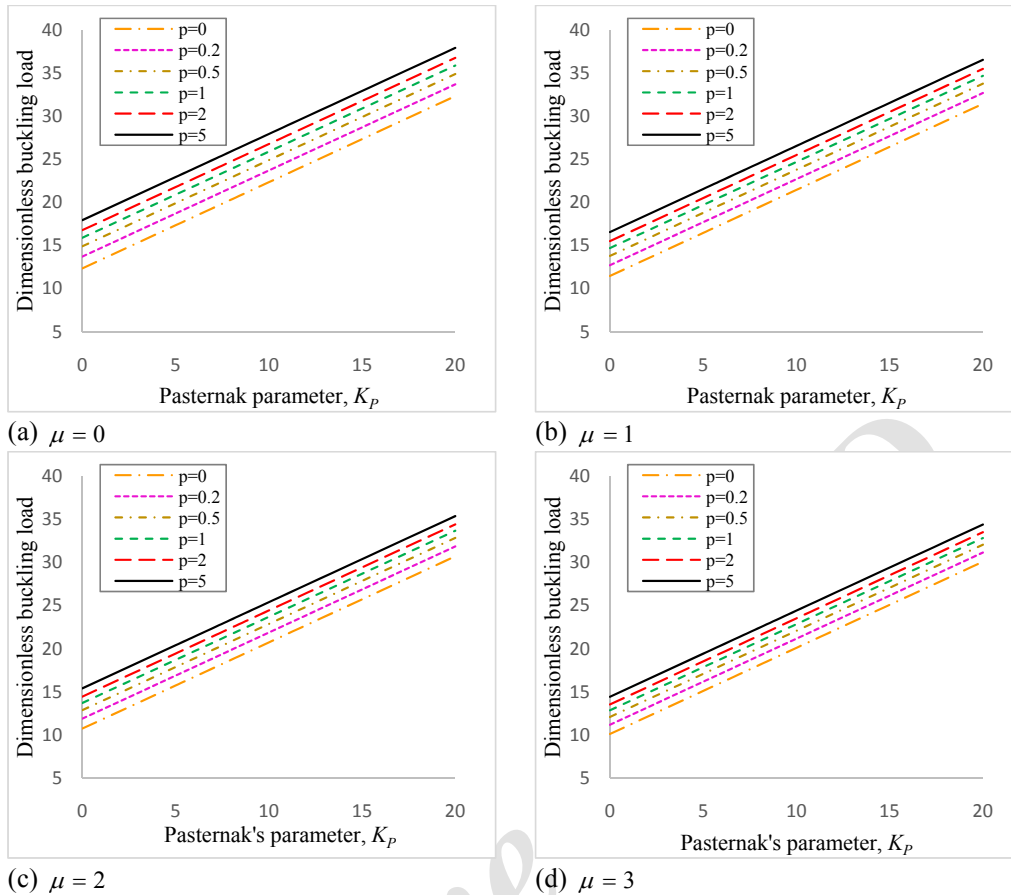


Fig. 6 (a, b, c, d). The variation of dimensionless buckling load of FG nanobeam with Pasternak's parameter and gradient index for different nonlocal parameters at  $L/h = 20$  and  $K_w = 25$ .

of Winkler's parameter dimensionless buckling load increases linearly for all values of gradient index. Also, it is observed that increasing gradient index yields the increment in dimensionless buckling load at constant Winkler's and nonlocal parameters.

The variation of the dimensionless buckling load of S-S FG nanobeam with respect to Pasternak's parameter  $K_p$  and different gradient indexes and nonlocal parameters is presented in Fig. 6(a-d). It is observed that with increase of Pasternak's parameter the dimensionless buckling load increases with a linear manner for all values of gradient index and nonlocal parameter. Also, it is seen that increasing gradient index results in increase of dimensionless buckling load at constant Pasternak's parameter. Comparing this figure with Fig. 5(a-d) specifies that the influence of Pasternak's parameter ( $K_p$ ) on non-dimensional buckling load is more significant than that of Winkler's parameter ( $K_w$ ).

## CONCLUSIONS

In the present work, buckling analysis of size-dependent FG nanobeams embedded in two-parameter elastic foundation is performed based on nonlocal TOSDBT in conjunction with Navier analytical method. Two types of mathematical models, namely, power law and Mori-Tanaka models are considered. The nonlocal governing differential equations in elastic medium are derived by implementing the minimum potential energy principle and using nonlocal constitutive equations of Eringen. Accuracy of the results is examined using available data in the literature. The effects of small scale parameter, material gradation, foundation parameters and slenderness ratio on buckling behavior of FG nanobeams are investigated. It is observed that, with an increase in Winkler's or Pasternak's parameter, the beam becomes more rigid and the dimensionless buckling load of FG nanobeams increases. Also, the presence of nonlocality has

a notable decreasing effect on the dimensionless buckling load of FG nanobeams, which shows the prominence of the nonlocal effect. So, it should be noted that reasonable selection of the value of the nonlocal parameter is also vital to ensure the accuracy of the nonlocal beam models. It must be pointed out that the PL and MT indexes have a remarkable effect on the buckling responses of FG nanobeam. Moreover, often the difference of the buckling loads between PL and MT models is very small, specifically at the range of lower gradient indexes. Thus, both material models reveal that with the increase of gradient index the buckling loads increase.

### CONFLICT OF INTEREST

The authors declare that there is no conflict of interests regarding the publication of this manuscript.

### REFERENCES

- [1] Iijima S., (1991), Helical microtubules of graphitic carbon. *Nature* 354: 56-58.
- [2] Eringen A. C., Edelen, D. G. B., (1972), On nonlocal elasticity. *Int. J. Eng. Sci.* 10: 233-248.
- [3] Eringen A. C., (1972), Nonlocal polar elastic continua. *Int. J. Eng. Sci.* 10: 1-16.
- [4] Eringen A. C., (1983), On differential equations of nonlocal elasticity and solutions of screw dislocation and surface waves. *J. Appl. Phys.* 54: 4703-4710.
- [5] Peddieson J., Buchanan G. R., Mc Nitt R. P., (2003), Application of nonlocal continuum models to nanotechnology. *Int. J. Eng. Sci.* 41: 305-312.
- [6] Reddy J. N., (2007), Nonlocal theories for bending, buckling and vibration of beams. *Int. J. Eng. Sci.* 45: 288-307.
- [7] Wang Q., Liew K. M., (2007), Application of nonlocal continuum mechanics to static analysis of micro-and nano-structures. *Phys. Let. A.* 363: 236-242.
- [8] Aydogdu M., (2009), A general nonlocal beam theory: Its application to nanobeam bending, buckling and vibration. *Phys. E.* 41: 1651-1655.
- [9] Pradhan S. C., Murmu T., (2010), Application of nonlocal elasticity and DQM in the flapwise bending vibration of a rotating nanocantilever. *Phys. E.* 42: 1944-1949.
- [10] Civalek Ö., Demir Ç., Akgöz B., (2010), Free vibration and bending analyses of cantilever microtubules based on nonlocal continuum model. *Math. Comput. Appl.* 15: 289-298.
- [11] Civalek Ö., Demir Ç., (2011), Bending analysis of microtubules using nonlocal Euler–Bernoulli beam theory. *Appl. Math. Model.* 35: 2053-2067.
- [12] Thai H-T., (2012), A nonlocal beam theory for bending, buckling, and vibration of nanobeams. *Int. J. Eng. Sci.* 52: 56-64.
- [13] Zenkour A. M., Abouelregal A. E., (2014), The effect of two temperatures on a FG nanobeam induced by a sinusoidal pulse heating. *Struct. Eng. Mech.* 51: 199-214.
- [14] Zenkour A. M., Abouelregal A. E., Alnefaie K. A., Abu-Hamdeh N. H., Aifantis E. C., (2014), A refined nonlocal thermoelasticity theory for the vibration of nanobeams induced by ramp-type heating. *Appl. Math. Comput.* 248: 169-183.
- [15] Zenkour A. M., Abouelregal A. E., (2014), Vibration of FG nanobeams induced by sinusoidal pulse-heating via a nonlocal thermoelastic model. *Acta Mech.* 225: 3409-3421.
- [16] Zenkour A. M., Abouelregal A. E., (2014), Nonlocal thermoelastic vibrations for variable thermal conductivity nanobeams due to harmonically varying heat. *J. Vibroeng.* 16: 3665-3678.
- [17] Zenkour A. M., Sobhy M., (2015), A simplified shear and normal deformations nonlocal theory for bending of nanobeams in thermal environment. *Phys. E.* 70: 121-128.
- [18] Zenkour A. M., Abouelregal A. E., (2015), Thermoelastic interaction in functionally graded nanobeams subjected to time-dependent heat flux. *Steel Compos. Struct.* 18: 909-924.
- [19] Zenkour A. M., Abouelregal A. E., Alnefaie K. A., Aljinaidi A. A., Abu-Hamdeh N. H., Aifantis E. C., (2015), State space approach for the vibration of nanobeams based on the nonlocal thermoelasticity theory without energy dissipation. *J. Mech. Sci. Tech.* 29: 2921-2931.
- [20] Zenkour A. M., Abouelregal A. E., Alnefaie K. A., Zhang X., Aifantis E. C., (2015), Nonlocal thermoelasticity theory for thermal-shock nanobeams with temperature-dependent thermal conductivity. *J. Therm. Stress.* 38: 1049-1067.
- [21] Zenkour A. M., Abouelregal A. E., (2015), Nonlocal thermoelastic nanobeam subjected to a sinusoidal pulse heating and temperature-dependent physical properties. *Microsys. Tech.* 21: 1767-1776.
- [22] Zenkour A. M., (2017), Nonlocal thermoelasticity theory without energy dissipation for nano-machined beam resonators subjected to various boundary conditions. *Microsys. Tech.* 23: 55-65.
- [23] Ke L-L., Wang, Y-S., (2011), Size effect on dynamic stability of functionally graded microbeams based on a modified couple stress theory. *Compos. Struct.* 93: 342-350.
- [24] Eltaher M. A., Emam S. A., Mahmoud F. F., (2013), Static and stability analysis of nonlocal functionally graded nanobeams. *Compos. Struct.* 96: 82-88.
- [25] Şimşek M., Yurtcu H. H., (2013), Analytical solutions for bending and buckling of functionally graded nanobeams based on the nonlocal Timoshenko beam theory. *Compos. Struct.* 97: 378-386.
- [26] Ebrahimi F., Ghadiri M., Salari E., Hoseini S. A. H., Shaghagh G. R., (2015), Application of the differential transformation method for nonlocal vibration analysis of functionally graded nanobeams. *J. Mech. Sci. Tech.* 29: 1207-1215.
- [27] Ebrahimi F., Salari E., (2015), Size-dependent free flexural vibrational behavior of functionally graded nanobeams using semi-analytical differential transform method. *Compos. B.* 79: 156-169.
- [28] Ebrahimi F., Salari E., (2015), A semi-analytical method for vibrational and buckling analysis of functionally graded nanobeams considering the physical neutral axis position. *CMES: Comput. Model. Eng. Sci.* 105: 151-181.
- [29] Niknam H., Aghdam M. M., (2015), A semi analytical approach for large amplitude free vibration and buckling of nonlocal FG beams resting on elastic foundation. *Compos. Struct.* 119: 452-462.
- [30] Pasternak P. L., (1954), On a new method of analysis of an elastic foundation by means of two foundation constants. *Gosudarstvennoe Izdatelstvo Literaturi po Stroitelstvu i*

- Arkhitecture, Moscow.*
- [31] Touratier M., (1991), An efficient standard plate theory. *Int. J. Eng. Sci.* 29: 901-916.
- [32] Rahmani O., Jandaghian A. A., (2015), Buckling analysis of functionally graded nanobeams based on a nonlocal third-order shear deformation theory. *Appl. Phys. A.* 119: 1019-1032.
- [33] Sahmani S., Aghdam M. M., Bahrami M., (2015), On the free vibration characteristics of postbuckled third-order shear deformable FGM nanobeams including surface effects. *Compos. Struct.* 121: 377-385.
- [34] Şimşek M., Reddy J. N., (2013), A unified higher order beam theory for buckling of a functionally graded microbeam embedded in elastic medium using modified couple stress theory. *Compos. Struct.* 101: 47-58.
- [35] Zhang B., He Y., Liu D., Gan Z., Shen L., (2014), Size-dependent functionally graded beam model based on an improved third-order shear deformation theory. *Eur. J. Mech. A/Solids.* 47: 211-230.
- [36] Sahmani S., Ansari R., (2013), Size-dependent buckling analysis of functionally graded third-order shear deformable microbeams including thermal environment effect. *Appl. Math. Model.* 37: 9499-9515.
- [37] Eltaher M. A., Emam S. A., Mahmoud F. F., (2012), Free vibration analysis of functionally graded size-dependent nanobeams. *Appl. Math. Comput.* 218: 7406-7420.
- [38] Rahmani O., Pedram O., (2014), Analysis and modeling the size effect on vibration of functionally graded nanobeams based on nonlocal Timoshenko beam theory. *Int. J. Eng. Sci.* 77: 55-70.

Archive of SID